Journal of Physics: Conference Series

Small-scale turbulent mixing at stratocumulus top observed by means of high resolution airborne temperature and LWC measurements

To cite this article: S P Malinowski *et al* 2011 *J. Phys.: Conf. Ser.* **318** 072013

Journal of Physics: Conference Series **318** (2011) 072013 doi:10.1088/1742-6596/318/7/072013

Small-scale turbulent mixing at stratocumulus top observed by means of high resolution airborne temperature and LWC measurements

S.P. Malinowski[1], K.E. Haman[1], M.K. Kopec[1], W. Kumala[1] and H. Gerber[2]

[1] Institute of Geophysics, Faculty of Physics, University of Warsaw, Poland
[2] Gerber Scientific Inc., Reston, VA, USA

E-mail: `malina@igf.fuw.edu.pl`

Abstract. High resolution measurements of temperature and cloud water, collected during Physics of Stratocumulus Top experiment are investigated. Two case studies presented here illustrate differences between "classical" stratocumulus capped with a sharp inversion and dry layer above and one type of "nonclassical" stratocumulus with weak inversion with moist air above. Entrainment and tranport into the cloud deck are investigated by means of statistical analysis of LWC and temperature fluctuations. It comes, that in "classical" case downdrafts with depleted water content are characterized with reduced temperature (effect of evaporative cooling, presumably negative buoyancy), while in this "non classical" case such downdrafts are of increased temperature, suggesting that in this case evaporative cooling is not a driving mechannism of downward transport.

1. POST: Physics of Stratocumulus Top research campaign

Physics of Stratocumulus Top (POST) was a research campaign held in the vicinity of Monterey Bay in July and August 2008 (Gerber *et al.*, 2010). High-resolution airborne measurements were focused on a detailed study of processes occurring at the interface between Stratocumulus capped atmospheric boundary layer and free troposphere. Research aircraft, equipped to measure thermodynamics, microphysics, dynamics and radiation, collected in-situ data porpoising around the cloud top. Information on the whole campaign, on flight patterns as well as on collected data are available in the open database http://www.eol.ucar.edu/projects/post/.

In this report we focus on a high-resolution measurements of temperature collected with the UFT-M thermometer (Kumala *et al.*, 2011) and liquid water content (LWC) measured with Particulate Volume Monitor PVM-100 (Gerber *et al.*, 1994). These sensors provided 1000 Hz (5.5 cm resolution) data. Due to close co-location of the fast-response instruments around the radome of the aircraft (Fig. 1), 40 Hz data ($\sim$1.4 m spatial resolution) can be directly compared as a representative for the sampling volume. In this respect POST differs from earlier research campaigns, where fast-response sensors were far apart (see e.g. Haman *et al.*, 2007).

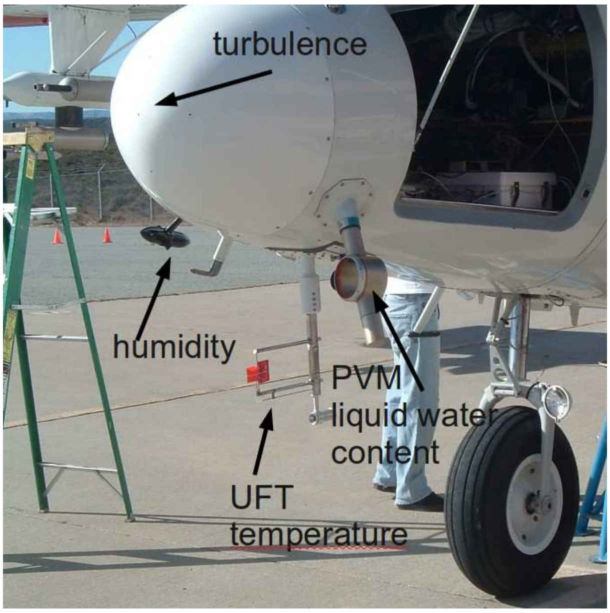

Figure 1. Radome of CIRPAS Twin Otter Research aircraft during POST. High frequency sensors measuring temperature (UFT), LWC (PVM), humidity and turbulence are closely co-located allowing to treat 40 Hz (∼1.4 m spatial resolution) data as representative for the same sampling volume.

2. Entrainment Interfacial Layer

Turbulence in a cloud layer causes entrainment of (almost) irrotational flow from free troposphere to atmospheric boundary layer. Entrained air is unsaturated and warm. Mixing with moist cloud results in evaporation of cloud water and cooling due to latent heat effect. Radiative fluxes at the cloud top result in strong cooling at the nighttime. Cooling and wind shear are local sources of turbulent kinetic energy in the cloud layer (see eg. Roode & Wang, 2007; Wang *et al.*, 2008; Kurowski *et al.*, 2009). Cooling also tends to stabilize layer above the cloud top. Turbulence, entrainment and mixing in the cloud top region depend on interplay between these effects.

Density gradient at the cloud top and nonlinearity of the evaporative cooling cause buoyancy of mixed volumes to vary, depending on thermodynamic parameters and mass proportions in each mixing event. Buoyancy sorting of mixed parcels leads to formation of the cloud-free and spatially and temporally variable Entrainment Interfacial Layer (EIL) separating the cloud top and free troposphere (Nicholls, 1989; Gerber *et al.*, 2005). The presence of EIL modifies dynamics and thermodynamics of entrainment. Empirical estimates of entrainment velocity based on a flux-jump method (Lilly, 1968) and on a method accounting for EIL are ambiguous (Stevens *et al.*, 2003). In the following we document two very different cases of RIL formation, illustrating problems which have to be overcome in order to parameterize entrainment velocity with more confidence.

3. Two cases: TO10 and TO13 flights

Flight TO10 was performed on 2008/08/04, 17:15-22:15 UTC. It was a daytime flight (local time is UTC -7h) through a fairly uniform cloud field. Typical vertical profiles (Fig.2) of liquid water potential temperature showed a strong inversion of about 10 K in 10 - 20 m thick layer. Cloud layeris identified in plots by differences between potential temperatures and by mixing ratios. The atmosphere above the cloud top is dry. A remarkable wind jump (∼4 m/s in u and v) occurs in a shallow layer separating cloud and free atmosphere.

Conditions during evening flight TO13, performed 2008/08/09, 00:58-06:00 UTC are different

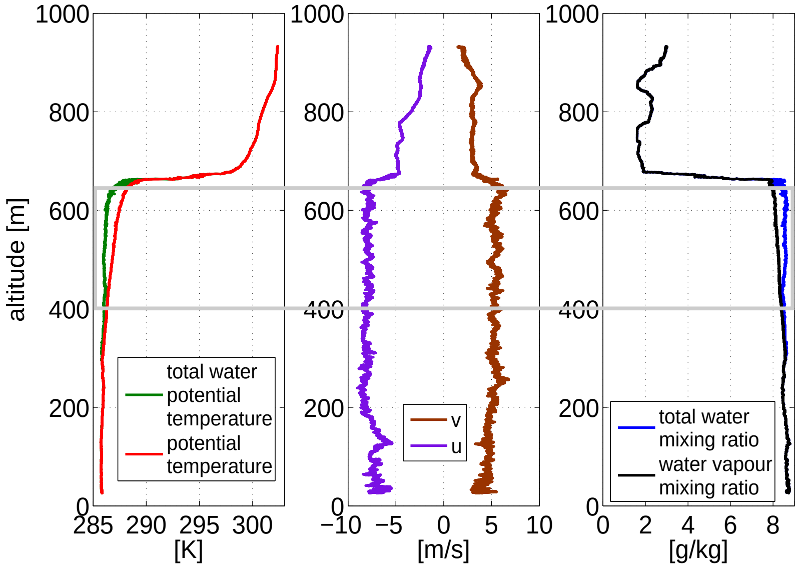

Figure 2. Vertical profiles of potential temperatures, wind components, water vapor and total water mixing ratios from TO10.

(Fig. 3). While total the strength of the inversion (~10 K) in 500 m thick layer above the cloud top is comparable to TO10, a sharp jump in a shallow layer above the cloud top is less than ~4 K. Wind shear (only v component) is substantially weaker due to increased thickness of the shear layer (~120 m). Water vapor mixing ratio above cloud top varies, but is high, indicating conditions close to saturation.

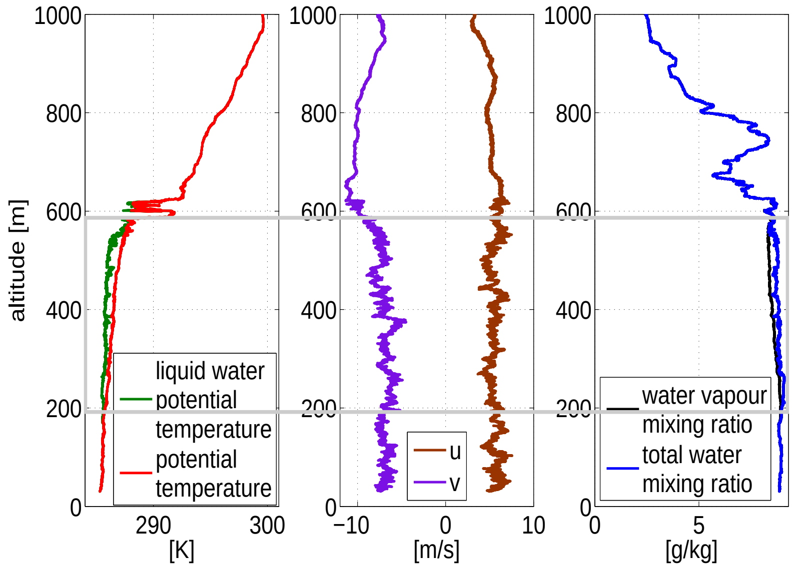

Figure 3. As in Fig. 2 but for TO13 case.

Figure 4 documents records of temperature, LWC and water vapour mixing ratio during typical descent into the cloud deck in course of flight TO10. Right panel in this figure presents 40 Hz data (∼1.4 m averages) of temperature and LWC plotted against the altitude. This profile reveals typical pattern of LWC characteristic for Sc under strong inversion: linear (almost adiabatic) increase of maximum LWC with altitude capped by a thin and sharp inversion layer (c.f. Fig 4 in Stevens, 2005).

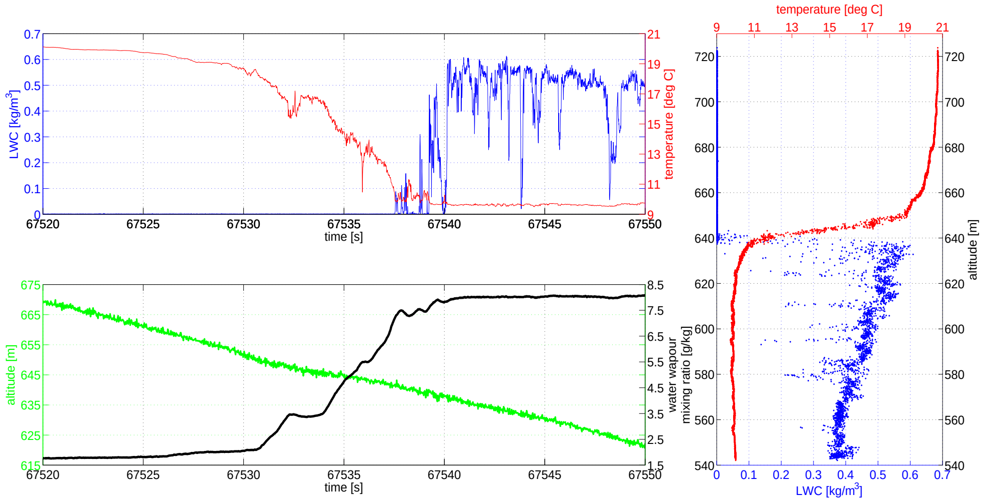

Figure 4. Typical records of thermodynamical parameters collected during descend with true air speed of 55 m/s into the cloud deck during TO10. Two left panels show LWC, temperature, water vapour mixing ratio and altitude as function of time. Each dot in the right panel corresponds to 0.01 s (55 cm long) average temperature and LWC plotted as function of altitude. Right panel presents LWC averaged over 1.4m long samples plotted against height.

Figure 5 presents analogous penetration of the cloud top from flight TO13. At a first glance the whole cloud top and inversion above looks different. There is no sign of linear increase of maximum LWC with altitude in the cloud top region. The level of inversion is ambiguous due to substantial temperature fluctuations in ∼40 m deep layer at the cloud top, which can be seen also in Fig. 3. It is worth mentioning, that similar structure of stratocumulus top was reported by Roode & Wang (2007).

4. Discussion

Comparison of Figs 4 and 5 leads to the conclusion that EIL in TO10 has different characteristics than in TO13. Substantial differences in inversion strength and humidity jump across inversion influence potential for evaporative cooling of the cloud top. For the TO10 case uniform mixtures of air from the cloud top and air from above inversion can be negatively buoyant, when mixed in adequate proportion (Randall, 1980; Deardorff, 1980). It means, that cloudy parcels of reduced LWC are likely to be removed from the mixing level down into the cloud and mixed layer.

In contrast the TO13 case mixing across the inversion never results in negative buoyancy. At high humidities latent heat effects are weak and affect buoyancy only marginally. In such a case most of the mixed parcels maintain diluted cloud water and remain on the level where mixing occurred, if not affected by other dynamical effects. The above explains observed differences in

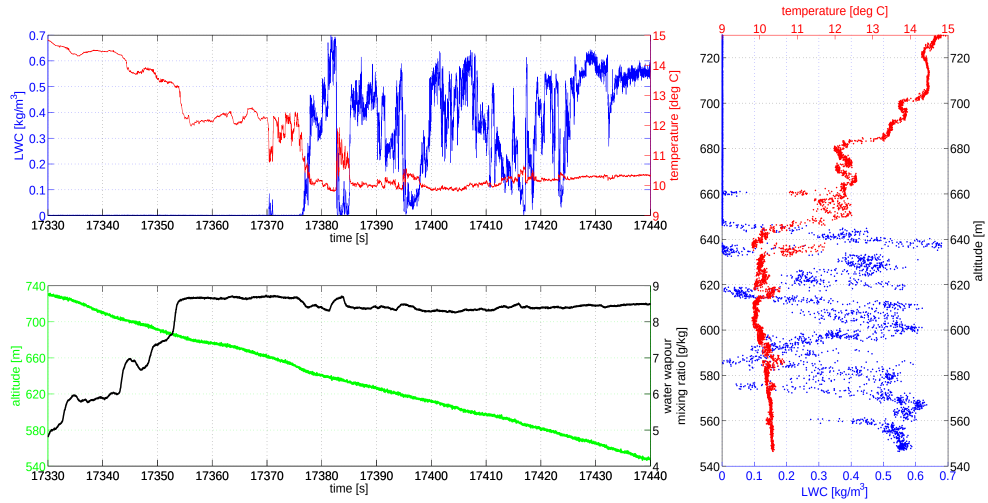

Figure 5. As in Fig. 4 but for TO13 case

LWC profiles.

In order to analyze buoyancy fluctuations in mixed parcels, PDF's of correlations of temperature and liquid water fluctuations inside the upper part of the cloud deck are analyzed (see Fig. 6). They are accompanied by PDF's of triple correlations (fluctuations of temperature, LWC and vertical velocity) in order to determine vertical transport in the cloud deck.

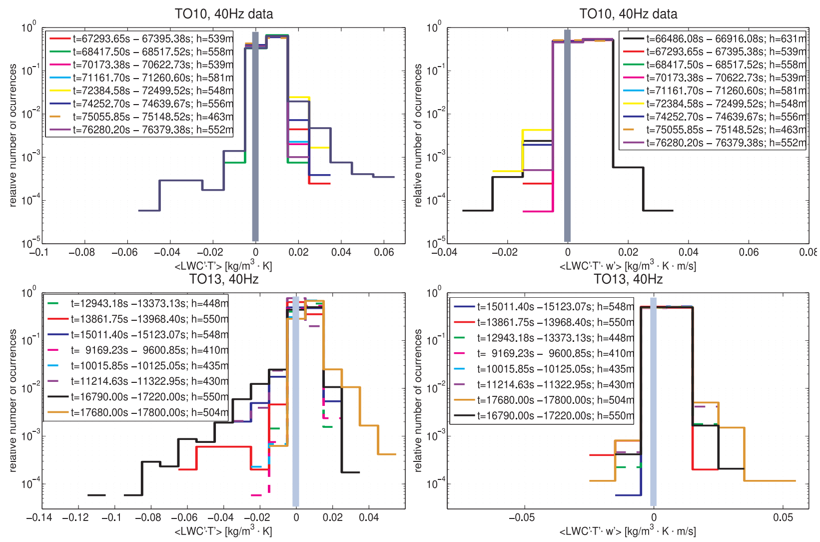

Figure 6. PDF's of double and triple correlations between temperature fluctuations (T'), LWC fluctuations (LWC') and vertical velocity (w') inside the cloud deck for TO10 (left) and TO13 (right).

In conditions similar to TO10 Gerber *et al.* (2005) found that air inside the cloud holes (regions of depleted LWC manifested as trenches or breaks in stratocumulus deck) is negatively buoyant. In such a case negative temperature fluctuations are correlated with negative LWC fluctuations (depleted LWC effects from evaporation and cooling) and negative vertical velocity (negatively buoyant downdraft). Numerical simulations by Kurowski *et al.* (2009) confirm that in such a case negative buoyancy of the air in cloud holes results from evaporative cooling during mixing. This picture agrees well with PDF's of double and triple correlations from TO10.

In contrast PDF's from TO13 indicate that cloud holes (depleted LWC) and downward motions are characterized with the increased temperature, which is illustrated in Fig. 7. Such correlations are possible only when downdrafts are not driven by buoyancy. We hypothesize that in TO13 case downdrafts result from larger-scale eddies due to mechanical production of TKE by the wind shear just above the cloud top. The density jump at the cloud top is too small to prevent deep mixing and the humidity jump is too small to enhance density differences by evaporative cooling. This hypothesis should be verified in the future with numerical modeling using the LES technique.

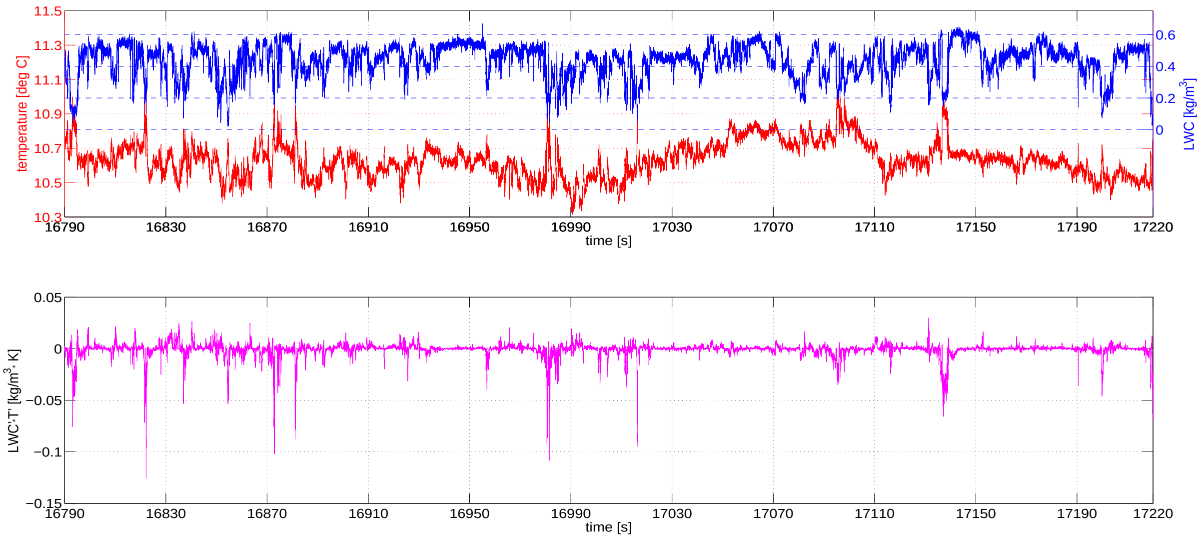

Figure 7. Upper panel: 100Hz (55cm spatial resoloution) LWC and temperature record on a horizontal segment of TO13 flight inside the cloud deck. Lower panel: correlations of LWC a T fluctuations.

ACKNOWLEDGMENTS: This research was supported by the National Science Foundation with the grant ATM-0735121 and by the Polish Ministry of Science and Higher Education with the grant 186/W-POST/2008/0. We thank all POSTers and CIRPAS crew for the collaboration during the field campaign.

References

Deardorff, J. W. 1980 Cloud-top entrainment instability. *J. Atmos. Sci.* **37**, 131–147.

Gerber, H., Arends, B.G. & Ackerman, A.S. 1994 A new microphysics sensor for aircraft use. *Atmos.Res.* **31**, 235–252.

Gerber, H., Frick, G., Malinowski, S. P., Brenguier, J.-L. & Burnet, F. 2005 Holes and entrainment in stratocumulus. *J.Atmos.Sci.* **62**, 443–459.

Gerber, H., Frick, G., Malinowski, S. P., Kumala, W. & Krueger, S. 2010 Post-a new look at stratocumulus. In *13th Conf. on Cloud Physics, Portland, OR*. American Meteorological Society, http://ams.confex.com/ams/13CldPhy13AtRad/techprogram/paper_170431.htm.

Haman, K. E., Malinowski, S. P., Kurowski, M. J., Gerber, H. & Brenguier, J.-L. 2007 Small scale mixing processes at the top of a marine stratocumulus - a case study. *Q.J.R.Meteorol.Soc.* **133**, 213–226.

Kumala, W., Haman, K. E., Kopec, M. K. & Malinowski, S. P. 2011 Ultrafast thermometer uft-m: High resolution temperature measurements during physics of stratocumulus top (post). Submitted.

Kurowski, M. J., Malinowski, S. P. & Grabowski, W. W. 2009 A numerical investigation of entrainment and transport within a stratocumulus-topped boundary layer. *Q.J.R.Meteorol.Soc.* **135**, 77–92.

Lilly, D. K. 1968 Models of cloud-topped mixed layers under a strong inversion. *Q.J.R.Meteorol.Soc.* **94**, 292–09.

Nicholls, S. 1989 The structure of radiatively driven convection in stratocumulus. *Q.J.R.Meteorol.Soc.* **115**, 487–511.

Randall, D. A. 1980 Conditional instability of the first kind upside-down. *J. Atmos. Sci.* **37**, 125–130.

Roode, S. R. & Wang, Q. 2007 Do stratocumulus clouds detrain? `FIRE I` data revisited. *Boundary-Layer Meteorol.* **122**, 479–491.

Stevens, B. 2005 Atmospheric moist convection. *Annu.Rev.Earth.Sci.* **33**, 605–643.

Stevens, B., Lenschow, D. H., Vali, G., Gerber, H., Bandy, A., Blomquist, B., Brenguier, J.-L., Bretherton, C. S., Burnet, F., Campos, T., Chai, S., Faloona, I., Friesen, D., Haimov, Laursen, K., Lilly, D. K., Loehrer, S. M., Malinowski, S. P., Morley, B., Petters, M. D., Rogers, D. C., Russell, L., Snider, V. Savic-Jovcic J. R., Straub, D., Szumowski, M. J., Thornton, H. Takagi D. C., Tschudi, M., Twohy, C., Wetzel, M. & van Zanten, M. C. 2003 Dynamics and chemistry of marine stratocumulus - `Dycoms II`. *Bull.Amer.Meteorol.Soc.* **84**, 579–593.

Wang, S., Golaz, J.-C. & Wang, Q. 2008 Effect of intense wind shear across the inversion on stratocumulus clouds. *Geophys.Res.Lett.* **35**, L15814.